CONF-881155--59

MECHANISMS OF CASCADE COLLAPSE

CONF-881155--59

DE89 009882

T. Diaz de la Rubia, K. Smalinskas, R. S. Averback, I. M. Robertson, H. Hseih
Department of Materials Science and Engineering
University of Illinois-Urbana
Urbana, IL 61801

and

R. Benedek
Materials Science Division
Argonne National Laboratory
Argonne, IL 60439

December 1988

/rlp
Distribution:
1-3. G. J. Hamilton
4. B. D. Dunlap
5. M. B. Brodsky
6. D. D. Koelling
7-12. Authors
13. Editorial Office

Submitted to the Proceedings of the MRS Fall Meeting on "Characterization of the Structure and Chemistry of Defects in Materials", Boston, MA, November 28-December 3, 1988.

*Work supported by the U.S. Department of Energy, BES-Materials Sciences, under Contract #W-31-109-ENG-38.

MECHANISMS OF CASCADE COLLAPSE

T. Diaz de la Rubia, K. Smalinskas, R. S. Averback, I. M. Robertson, H. Hseih
Department of Materials Science and Engineering
University of Illinois-Urbana
Urbana, IL 61801

and

R. Benedek
Materials Science Division
Argonne National Laboratory
Argonne, IL 60439

December 1988

Submitted to the Proceedings of the MRS Fall Meeting on "Characterization of the Structure and Chemistry of Defects in Materials", Boston, MA, November 28-December 3, 1988.

MECHANISMS OF CASCADE COLLAPSE

*T.Diaz de al Rubia, *K. Smalinskas, *R.S. Averback, *I.M.Robertson, *H. Hseih and **R. Benedek
*Department of Materials Science and Engineering, University of Illinois at Urbana-Champaign
**Materials Science Division, Argonne National Laboratory, Argonne, Il. 60439

ABSTRACT

The spontaneous collapse of energetic displacement cascades in metals into vacancy dislocation loops has been investigated by molecular dynamics (MD) computer simulation and transmission electron microscopy (TEM). Simulations of 5 keV recoil events in Cu and Ni provide the following scenario of cascade collapse: (i) atoms are ejected from the central region of the cascade by replacement collision sequences; (ii) the central region subsequently melts; (iii) vacancies are driven to the center of the cascade during resolidification where they may collapse into loops. Whether or not collapse occurs depends critically on the melting temperature of the metal and the energy density and total energy in the cascade. Results of TEM are presented in support of this mechanism.

INTRODUCTION

Irradiation of a metal or semiconductor with energetic particles, ions or fast neutrons, leads to production of point defects. The motion of these defects enhance various diffusional processes, ion beam mixing, segregation, phase transformations and grain growth. In addition, the retention of defects in semiconductors is often detrimental to device efficiency. An understanding of the response of a material requires the determination of both the number and configuration of point defects created by the irradiation. In the past several years it has been established that vacancies produced in energetic displacement cascades often condense into dislocation loops during the evolution of the cascade event, even when the irradiations are performed at low temperatures where vacancies are immobile [1]. In attempting to explain this behavior, it had been noted that the probability for such "cascade collapse" correlated closely with ion beam mixing thus suggesting a role of thermal spikes in the collapse process [2]. In this work, the role of thermal spikes in cascade collapse has been studied further using molecular dynamics (MD) computer simulations and transmission electron microscopy observations of loop collapse in Kr irradiated CuNi alloys.

COMPUTER SIMULATIONS

Simulation model: Molecular dynamics computer simulations were employed to follow the evolution of the cascade structure from the time of initiation of a recoil event to a state of near quiescence. The MD code employed for these calculations is a modified version of SUPERGLOB [3], the details of which are published elsewhere [4]. Briefly, SUPERGLOB employs fixed boundary atom positions and up to ≈ 180,000 movable atoms. Two layers of atoms contiguous with the boundary are damped to minimize the reflection of outward directed energy thus simulating an infinite crystal. Two types of simulation were employed, a primary knock-on atom recoil event (PKA) and a heat spike. The former is initiated by setting the kinetic energy of one lattice atom equal to the entire cascade energy and the others equal to zero. The initial atomic positions are the perfect lattice sites. A heat spike is generated by partitioning the initial cascade energy among all of the atoms in the cascade volume according to a Maxwellian distribution; the temperature gradient is smoothed by lowering the temperature of the surrounding few shells of atoms. The initial positions of the atoms are also perfect lattice sites. The volume of the cascade was estimated from the results of the PKA simulation. The lattice temperature for both events is 0 K.

Pair potentials were employed for most of the calculations. Cu was represented by the Gibson II form of a Born-Meyer potential [5] and Ni by the Johnson-Erginsoy potential [6]. These potentials are very short range, cutting off to zero between the first and second nearest neighbor position. Although these short range pair potentials are somewhat idealistic, their computational efficiency is important for simulations of high energy events. Both the Cu and Ni pair potentials provide reasonable values for point defect properties, threshold displacement energies and elastic constants [6,7]. A few heat spike events were run using potentials derived by the embedded atom method [8]. These events serve as a calibration for the pair potentials.

Results: Figure 1 shows the final configuration of the point defects that were produced by a 5 keV PKA in Cu. The self-interstitial atoms (filled circles) are distributed on the periphery of the cascade whereas the vacancies (open circles) form a compact cluster at the center of the cascade. Although the vacancies have not collapsed into a dislocation loop in this event nor have they in other 5 keV simulation events, their formation of a cluster in the central core of the cascade appears to represent the rudiments of cascade collapse. Higher energies or greater energy densities are probably necessary for actual collapse. It is noteworthy that cascade collapse arising from a single ion impact in Cu has only been observed experimentally when the ion energies were greater than ≈ 10 keV. Understanding how vacancies collapse into a dislocation loop, thus begins with understanding how vacancies condense into the cluster shown in Figure 1.

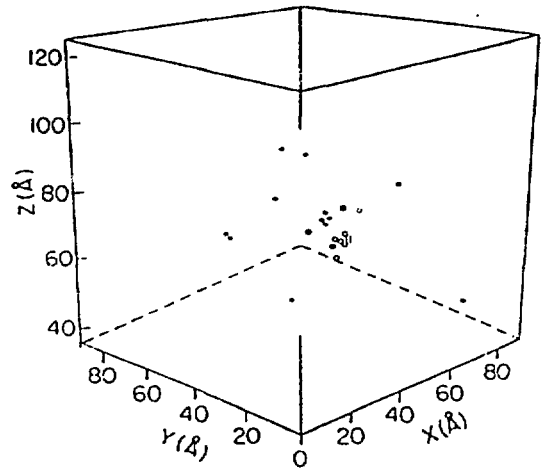

Fig. 1 Final arrangements of point defects produced by a 5 keV PKA. (o) vacancies; (•) SIA's.

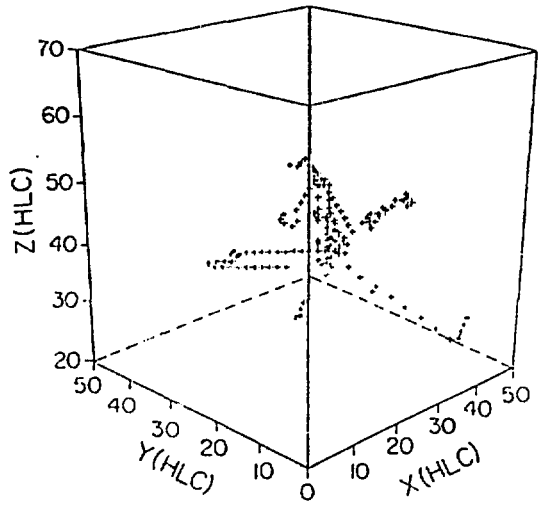

Fig. 2 Replacement sequences leading to final positions of SIA's. (HCL is half lattice constant, 1.8 Å in Cu.)

Vineyard and co-workers demonstrated for low energy recoil events, T < 400 eV, that Frenkel pairs are created via replacement collision sequences along close packed directions, (110) and (100) in fcc metals and (111) in bcc metals [5,6]. Figure 2 shows that the same mechanism is responsible for defect production in energetic displacement cascades. Linear trails of replacement sequences are shown leading to the positions of the SIA's. It can also be seen that: 1) there is a tendency for SIA's to cluster on the periphery of the cascade owing to their strong elastic interaction, and 2) that SIA's are excluded from the central core of the cascade. Unlike defect production at low energies, the positions of vacancies in the cascade are not the sites where the replacement chains leading to SIA formation were initiated, but rather have migrated some distances away during a later phase of the cascade.

A primary result of our MD simulations is the observation of local melting in the central core of the cascade [9]. Melting was deduced from a comparison of the density, temperature and pair correlation function (g(r)) of the cascade core with corresponding quantities in liquid Cu. Some of this evidence is illustrated for Cu in Figures 3a and 3b which show a cross sectional view of atoms in a thin slab of material of thickness $a_0/2$ through the center of the cascade, 3a,

and g(r) for atoms in the cascade region, 3b. Clearly apparent in Figure 3a is a disordered region in the center of the cascade; it has a remarkably sharp interface with the surrounding crystalline material. Noteworthy in the pair correlation function is the absence of a (200) peak at 3.6 Å found in crystalline, but not liquid, Cu. The melt in the cascade event in Cu persists for several picoseconds (ps) so that several lattice vibrations occur during the period of excitation. Point defects located in the melt, which has a density ≈ 85% that of crystalline Cu, can lose their distinct identity during this time. From this picture of cascade melting, we suggest the following mechanism for cascade collapse. As the cascade melt cools, it begins to solidify at the cooler periphery. Initially, density fluctuations in the melt are small and resolidification proceeds with perfect epitaxial regrowth. The density fluctuations increase as the cascade volume shrinks, owing to the loss of atoms earlier in the cascade evolution by replacement collision sequences. Eventually, these mass fluctuations freeze out as vacancies. The precise number of vacancies in this region and their degree of clustering depend on the number of RCS's extending beyond the melt boundaries and the speed of the resolidification front. For metals with higher melting temperatures than Cu, such as Ni, the front moves more rapidly and the sweeping of vacancies to the center of the cascade is less pronounced. For metals of lower melting temperatures, or for cascades of higher energy, the clustering of vacancies is expected to be even more important. Protasov and Chudinov have proposed a similar mechanism of collapse based on the thermomigration of vacancies toward the center of the cascade driven by the steep radial temperature gradient [11].

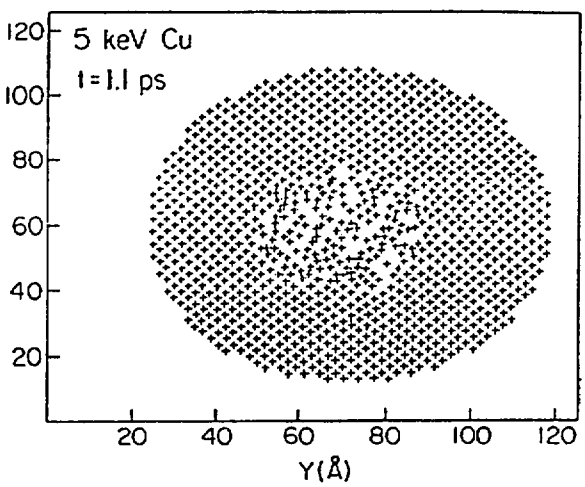

Fig. 3a: Projection of a (100) cross sectional slab of thickness $a_0/2$ near the center of a 5 keV cascade at t = 1.1ps.

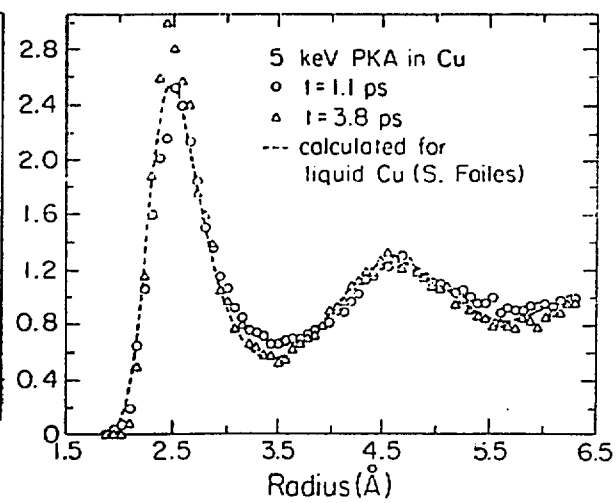

Fig. 3b: Radial pair correlation functions of atoms in the disordered zones at two times. Results for liquid Cu (10) are also shown.

Additional evidence for our scenario of cascade collapse has been garnered from MD simulations of heat spike events. For these simulations, an arbitrarily chosen vacancy concentration of 2 at.% is distributed randomly within the volume of the heat spike. The simulation is run until all vacancy motion has ended, 5 - 10 ps. The influence of energy density on cascade collapse was studied by increasing the energy of the cascade but maintaining the same initial cascade volume. The data from these simulations of cascades in Cu and Ni are compiled in Table 1. The positions of the vacancies are represented by their radius of gyration, r_g about the centroid of the vacancy distribution. It is observed in Cu, that r_g decreases with increasing energy density. The decrease of r_g in Ni is far smaller. The large contrast between Cu and Ni, we believe, derives mainly from their different melting temperatures. We note that the higher energy collisions indigenous to a real cascade play no role in the heat spike simulations, and thus apart from establishing the initial conditions for the thermal spike, the collision cascade does not appear important for cascade collapse.

Although the current simulations reveal the importance of local melting in cascade collapse, it is

reasonable to question the reliability of the pair potentials employed in the calculations for describing "real" Cu and Ni. Since melting appears to play a dominant role in cascade collapse, we have examined the melting temperatures predicted by the Gibson II and Johnson-Erginsoy potentials. Our preliminary values of melting temperature are 1100 K and 2400 K for Cu and Ni respectively [12], and thus the differences we report for cascades in Cu and Ni may exaggerate, somewhat, their true behavior. We have also begun heat spike simulations using potentials derived from the embedded atom method. These data are also included in table 1. It can be seen that the qualitative behavior in Cu is the same for the two potentials, but as expected from the higher melting temperature of Cu derived from the embedded atom method potentials [13] than from the Gibson II potential, the contraction of the vacancy distribution is smaller for the embedded atom potentials. Whether or not the smaller radius of gyration observed for the EAM potentials at 2.9 eV/atom indicate a greater vacancy binding energy for these potentials or a statistical variation can not be answered until more events are run.

Table 1. Radius of gyration of the vacancy distribution before and after a heat spike.

energy density	1.1 eV/atom	2.9eV/atom
Cu (Gibson II)	16.35 Å - 10.61 Å	16.35 Å - 9.62 Å
Cu (EAM)	16.37 Å - 14.79 Å	16.38 Å - 7.81 Å
Ni	16.40 Å - 15.99 Å	

ELECTRON MICROSCOPY

Experimental methods: Transmission electron microscopy has been used to investigate the damage structure produced in a series of CuNi alloys by room temperature irradiations to a dose of 5 x 10^{11} ions cm^{-2} with 50 keV Kr ions. The CuNi system was selected for this study since these metals have nearly the same atomic number and atomic size as well as the same crystal structure. Cu and Ni, moreover, are miscible across the entire composition range. The melting temperature of CuNi alloys, however, increases monotonically from 1325 K for pure Cu to 1725 for pure Ni. Thus, this system provides a means to systemmatically vary the melting temperature without varying the kinematics of the collision cascade in any appreciable way. The response of the alloy to the irradiation was determined from measurements of the defect yield, which is defined as the number of visible vacancy loops created per incident ion, and by the size of the defect. The loop yield is determined from micrographs taken with the (200) type reflections. This diffraction vector images all possible Frank loops (Burgers vector a/3<111>) and 2/3 of the possible perfect loops (Burgers vector a/2<110>). In addition to determining the defect yield, the size of the dislocation loop was determined. The loop size is measured as the length of the interface in black-white lobe images and as the maximum dimension of black dot images; Saldin et al [14] have shown that these sizes correspond approximately to the size of the actual defect. The average number of vacancies retained in dislocation loops, the loop efficiency, can then be determined.

Results The most cogent experimental results are illustrated in Figure 4 which shows the number of vacancies contained in loops per incident 50 keV Kr^+ ion, i.e., the product of loop yield and average number of vacancies per loop, as a function of alloy melting temperature. Also shown are the defect yields. The trend of decreasing vacancy accumulation in loops with increasing melting temperature is apparent. The defect yields also follow this trend, although the defect yield appears to be as high for the dilute NiCu alloy as for pure Ni even though the melting temperature is lower. The experimental error is deemed too small to alter this conclusion. This latter result indicates that, at least in dilute alloy systems, melting temperature is not the sole materials variable controlling loop collapse even though it may be the most important. It must be emphasized at this point, however, that these preliminary experiments were performed at room temperature which is above stage III (vacancy migration stage) in Cu, but below it in Ni. Comparison of the loop yields produced in other systems by irradiation at

room temperature and 30 K show that loop collapse still occurs at the lower temperature, but with a reduced probability. The trend observed in the room temperature irradiations of the CuNi alloys is therefore expected to persist when the irradiations are performed below stage III .

Measurement of dependence of defect yield on ion fluence provides additional evidence for the importance of cascade melting in cascade collapse. In situ measurements of cascade collapse in Ni irradiated at 30 K with 50 keV Ni^+ ions reveal that some loops produced by irradiation disappear during subsequent irradiation. The probability for loop annihilation increases at a rate proportional to loop concentration. Loop loss may occur by loops slipping to the foil surface or by the direct impact by a second displacement cascade. Loop loss to the surface cannot account for all loops lost as the majority of loops produced in these systems are sessile undissociated, partially dissociated and dissociated Frank loops. Elimination of a loop by direct impact of a second displacement cascade can be understood assuming cascade melting as follows. As described above, point defects produced in a cascade are delocalized in the cascade melt and only relocalize during solidification. When a new cascade overlaps a previously created loop, those vacancies in the loop are absorbed in the new melt, and they must subsequently recondense during resolidification for the loop to reappear. This should occur with a probability roughly equal to the cascade yield. In Ni the yield is low, and thus, most loops which fall within the melt zone of a later cascade are likely to be annihilated. For metals with high cascade yields, like Ag or Au, loop annihilation is expected with much reduced frequency. Measurements in these systems have not yet been carried out.

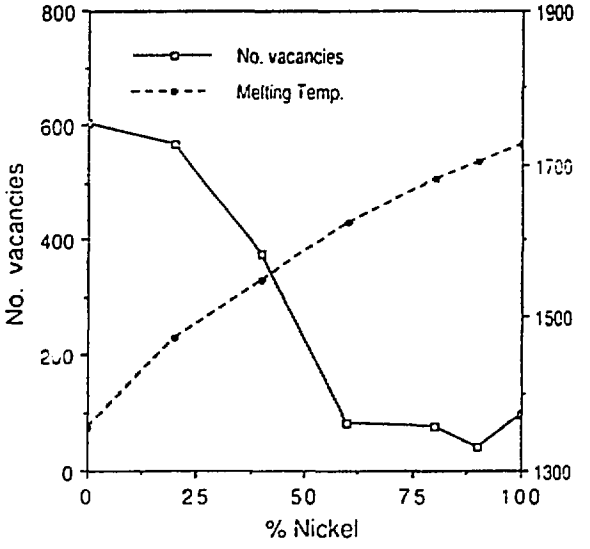

Fig. 4 (a) Number of vacancies contained in loops per incident ion.

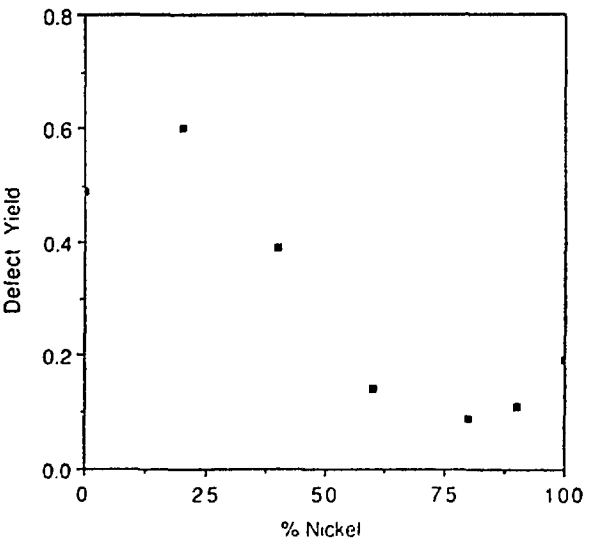

Fig. 4 (b) Loop yields in CuNi alloys.

ACKNOWLEDGMENTS

This work was supported by the Department of Energy, Basic Energy Sciences under grants, DE-AC02-76ER01198 and W-31-109-ENG-38 at the University of Illinois and Argonne, respectively.

REFERENCES

1. see, e.g., C.A. English and M.L. Jenkins, Mats. Science Forum, 15-18, 1003 (1987).
2. R.S. Averback and D.N.Seidman, Mats. Science Forum, 15-18, 963 (1987)
3. SUPERGLOB was originally developed by Prof. J.R. Beeler Jr. at North Carolina State

University.
4. W.E. King and R. Benedek, J. Nucl. Mater. 117, 26 (1983).
5. J.B. Gibson, A.N. Goland, M. Milgram and G.H. Vineyard, Phys. Rev. 120, 1229 (1960).
6. C. Erginsoy, G.H. Vineyard and A. Englert, Phys. Rev. 120, 1229 (1960).
7. R.A. Johnson, Phys. Rev. 145, 423 (1966).
8. M.S. Daw and M.I. Baskes, Phys. Rev. B29, 6443 (1984).
9. T. Diaz de la Rubia, R.S. Averback, R. Benedek and W.E. King, Phys. Rev. Lett. 59, 1930 (1987).
10. S. Foiles, Phys. Rev. B32, 3409 (1985).
11. V.I. Protasov and V.G. Chudinov, Radiat. Effs. 66, 1 (1982).
12. H. Hsieh, R.S. Averback and R. Benedek, unpublished result.
13. J. Adams, private communication
14. D.K.Saldin, A.Y.Stathopoulos and M.J.Whelan, Phil. Trans. Roy. Soc. 292, 513 (1979).